New Insights into Neuroblastoma Cisplatin Resistance: A Comparative Proteomic and Meta-Mining Investigation

ARTICLE *in* JOURNAL OF PROTEOME RESEARCH · FEBRUARY 2011

Impact Factor: 4.25 · DOI: 10.1021/pr100457n · Source: PubMed

10 AUTHORS, INCLUDING:

Luisa Pieroni
University of Rome Tor Vergata-S.Lucia Fo…
32 PUBLICATIONS **682** CITATIONS
SEE PROFILE

Antonella Roveri
University of Padova
71 PUBLICATIONS **4,196** CITATIONS
SEE PROFILE

Mattia Zaccarin
University of Padova
14 PUBLICATIONS **69** CITATIONS
SEE PROFILE

Valeria Marzano
Catholic University of the Sacred Heart
26 PUBLICATIONS **390** CITATIONS
SEE PROFILE

research articles Journal of proteome research

New Insights into Neuroblastoma Cisplatin Resistance: A Comparative Proteomic and Meta-Mining Investigation

Simona D'Aguanno,[†,‡] Annamaria D'Alessandro,[†,‡] Luisa Pieroni,[†,‡] Antonella Roveri,[§] Mattia Zaccarin,[§] Valeria Marzano,[†,‡] Michele De Canio,[†] Sergio Bernardini,[†] Giorgio Federici,[†,‡] and Andrea Urbani*[,†,‡]

Department of Internal Medicine, University of Rome Tor Vergata, Rome, Italy, S. Lucia Foundation - IRCCS, Rome, Italy, and Departement of Biological Chemistry, University of Padova, Padova, Italy

Received May 14, 2010

Neuroblastoma is one of the most aggressive solid tumors in the childhood. Therapy resistance to anticancer drugs represents the major limitation to the effectiveness of clinical treatment. To better understand the mechanisms underlying cisplatin resistance, we performed a comparative proteomic study of the human neuroblastoma cell line SH-SY5Y and its cisplatin resistant counterpart by both the classical 2-DE electrophoresis coupled to mass spectrometry and the more innovative label-free nLC−MS^E. The differentially expressed proteins were classified by bioinformatic tools according to their biological functions and their involvement in several cellular processes. Moreover, a meta-mining investigation of protein ontologies was also performed on available data from previously published proteomics studies to highlight the modulation of significant cellular pathways, which may regulate the sensitivity of neuroblastoma to cisplatin. In particular, we hypothesized a major role of the transcription factor nuclear factor-erythroid 2-related factor 2 (Nrf2) pathway. Confocal microscopy experiments, enzyme assay, and Western blotting of proteins regulated by Nrf2 provided evidences that this pathway, playing a protective role in normal cells, may represent a potential novel target to control cisplatin resistance in neuroblastoma.

Keywords: cisplatin • neuroblastoma • chemoresistance • 2-DE, label-free LC−MS • Nrf2

Introduction

Neuroblastoma is the most common extracranial neoplasm diagnosed during the childhood.[1] A minimal number of neuroblastoma tumors regress spontaneously, while in the majority of the cases, the development of a malignant clinical phenotype characterized by aggressive metastasis[2] results in an elevated mortality of more than 50% of the chemoradiotherapy-treated patients.[3] Among the anticancer drugs used for the treatment of neuroblastoma, one of the most common is cis-diamminedichloroplatinum(II) (cisplatin, cDDP), the first platinum-based molecule introduced in clinical chemotherapy.[4] In the cytoplasm, water molecules replace the *cis*-chloro ligand of the compound, enabling it to react toward nucleophilic centers of DNA, RNA, proteins and membrane phospholipidis.[5] Unfortunately, the effectiveness of this anticancer molecule is limited by resistance development. A wide range of mechanisms are supposed to be involved in this clinical relevant phenomenon: (I) reduced intracellular platinum concentration due to modulation of drug uptake or efflux; (II) increased association of cisplatin to glutathione (or increased efflux of the cisplatin-glutatione complex) combined to elevated activities of phase 2 detoxification enzymes; (III) increased repair of DNA−cisplatin adducts; and (IV) modulation of apoptotic pathways.[6,7] Nevertheless, a definitive understanding of the rise in cisplatin resistance has not been reached yet. The proteomic platform represents a powerful tool to perform high-throughput studies, allowing the detection of modulated proteins from a variety of samples. Several proteomic studies considerably contributed to collect a large amount of data about possible mechanisms underlying cisplatin resistance in different cell models[8] and characterization of neuroblastoma cell lines.[9,10] To identify and characterize more determinants of cisplatin resistance, we performed a global quantitative proteomic analysis of a neuroblastoma sensitive cell line and its resistant counterpart by two complementary proteomic approaches: the classical 2-DE electrophoresis coupled to mass spectrometry joined to the more innovative nLC−MS^E. The resulting gene ontology meta-mining revealed the modulation of different cellular processes, which may regulate the sensitivity of neuroblastoma to cisplatin. In particular, we hypothesized a major common role of the transcription factor nuclear factor-erythroid 2-related factor 2 (Nrf2) pathway in the emergence of cisplatin resistance.

Nrf2 is a member of the basic leucine zipper (bZIP) transcription factor subfamily displaying a Cap 'n Collar motif.[11] Under basal conditions, Nrf2 molecules are predominantly sequestrated in the cytoplasm by Kelch-like ECH-associated

* To whom correspondence should be addressed. Prof. Andrea Urbani, Dept. of Internal Medicine, University of Rome "Tor Vergata", Via Montpellier 1, 00133 Roma (I). FAX: +39-06-501703332. E-mail: andrea.urbani@uniroma2.it.
† University of Rome Tor Vergata.
‡ S. Lucia Foundation.
§ University of Padova.

10.1021/pr100457n

Published on Web 12/04/2010

protein 1 (Keap1).[12] Keap1 is also identified as a substrate adaptor for Cullin-dependent E3 ubiquitin ligase complex, which targets Nrf2 for ubiquitination and consequent proteasomal degradation.[13] Chemical and/or oxidative stress conditions disrupt the Nrf2/Keap1 complex, leading Nrf2 to translocate into the nucleus to form heterodimers with other bZIP transcription factors named Maf proteins.[14] Upon heterodimerization Nrf2 specifically binds to a *cis*-acting enhancer called antioxidant responsive element (ARE) of the promoter of many antioxidant and phase II detoxification genes.[15−17]

Here we provided evidences that the Nrf2 pathway, playing a protective role in normal cells, may be a potential novel target to control cisplatin resistance in neuroblastoma.

Materials and Methods

Cell Culture. The human neuroblastoma (NB) cell line SH-SY5Y was maintained in DMEM High glucose (GIBCO, Paisley, U.K.) containing 10% bovine serum albumin (FBS) (GIBCO), 2 mM L-glutamine (GIBCO), 1% NEAA (GIBCO), 1% sodium pyruvate (GIBCO), 10 mM HEPES (GIBCO) and 1% antibiotics (100 U/mL penicillin/streptomycin) (GIBCO) under standard conditions (37 °C temperature, 5% CO_2 in a humidified atmosphere). The SH-SY5Y cell line resistant to cisplatin (SIGMA, St. Louis, MO) was selected treating cells with increasing concentration of drug starting from 1 nM to 1 μM (0.3 μg/mL). Preparations of cell lysates for proteomic analysis were repeated in identical conditions of cell growth, 48 h after cell plating when cells reached a 80−90% confluence in 100 × 20 mm culture disks in complete media.

MTT Assay. NB cell lines were seeded at 1.5×10^4 cells/well in 96 well flat-bottom plates and cultured for 24 h in 100 μL of complete medium. After 24 h, media were replaced with fresh media containing vehicle (DMSO) or cisplatin at different concentration and cells were left at 37 °C for other 24 h. Then cells were washed with PBS (SIGMA) and 100 μL of a 3-(4,5-dimethylthiazol-2-yl)-2,5-diphenyltetrazolium bromide (MTT, SIGMA) solution (0.5 mg/mL) were added to each well and cells were incubated for 4 h. Formazan crystals were dissolved by adding 100 μL of solubilization solution (TOX-1 kit, SIGMA) and after 1 h absorbance was measured at 570 nm subtracting 690 nm. A well containing 100 μL of MTT solution (0.5 mg/mL) plus 100 μL of solubilization solution was used as blank. Experiments were performed in triplicate. OD values were normalized versus starting point value when added drug is zero and viability is maximum. Statistical analysis was performed by Student's *t* test. The results were analyzed and the logEC50 values (EC50 is the drug concentration that produces 50% of the maximum possible response) were determined with the GraphPad Prism analysis software package (Graph-Pad Software, San Diego, CA) using nonlinear regression (sigmoidal dose response, variable slope).

Cell Lysis. Cells were harvested in cold PBS and centrifuged. Protein extraction for 2D-electrophoresis was performed by sonication in a sample buffer (SB) containing 7 M urea, 2 M thiourea, 50 mM DTT, 4% (w/v)CHAPS, 40 mM Tris, 0.5% (v/v) ampholytes in the presence of protease inhibitor cocktail. After incubation at 36 °C for 1 h samples were centrifuged at 13,000 rpm for 30 min. Supernatants were collected and protein concentration was determined using an adapted TCA procedure.[18] For nuclei enrichment cells were dissolved in 200 μL of lysis buffer (10 mM HEPES, pH 7.9, 1.5 mM $MgCl_2$, 10 mM KCl, 0.5 mM DTT, in the presence of protease inhibitor cocktail (Sigma), 20 ng/μL DNase and 20 ng/μL RNase) and incubated on ice for 30 min. After incubation, NP-40 (Roche, Basel, Switzerland) was added at final concentration of 0.5% (v/v). Samples were mixed by vortexing and centrifuged at 13 000× *g* for 5 min at 4 °C. Supernatant was recovered and stored as cytosol fraction. The pellet was dissolved in SB, in the presence of protease inhibitor cocktail, 20 ng/μL Dnase and 20 ng/μL Rnase, incubated 30 min at 36 °C, sonicated, and centrifuged 13 000× *g* for 30 min.

2-D Electrophoresis. Three independent protein extractions were carried out from SH-SY5Y wt and SH-SY5Y cisplatin cell lines. One-hundred micrograms of pooled extractions from SH-SY5Y wt and SH-SY5Y cisplatin cell lines were precipitated by adding a mix of ethanol, methanol, and acetone (ratio 2:1:1, v/v) and then dissolved in SB. Then rehydration buffer (6 M urea, 2 M thiourea, 15 mM DTT, 4% (w/v) CHAPS, 0.5% (v/v) IPG-buffer (pH 3−10 NL, Amersham Biosciences, Buckinghamshire, U.K.) and bromophenol blue in traces) was added until a final volume of 350 μL. Isoelectric focusing was performed in an IPGphor system (Amersham Biosciences) using Immobiline Dry strips 18 cm, pH interval 3−10 nonlinear at 20 °C. After 8 h of passive and 8 h of active rehydratation at 30 V, proteins were focused by holding at 100 V for 1 h, ramping to 300 V over 1 h, holding at 300 V for 1 h, ramping to 3500 V over 3 h, holding at 3500 V for 1 h, successively ramping to 8000 V over 3 h and plateau at 8000 V until 50 000 V/h. Prior to perform the second dimension, focused IPG strips were equilibrated for 15 min in the equilibration buffer (6 M urea, 2% (w/v) SDS, 30% (v/v) glycerol, 50 mM Tris-HCl, pH 8.8) containing 1% (w/v) DTT and for 15 min in the same buffer supplemented with 4% (w/v) iodoacetamide. The second dimension was performed on 7−14% polyacrylamide gradient gels using a PROTEAN Plus Dodeca cell (Bio-Rad, Hercules, CA) at 20 mA/gel for 1 h and at 50 mA/gel until the end of the run. After the run, gels were incubated in a fixing solution (50% (v/v) methanol, 12% (v/v) acetic acid, 0.05% (v/v) formaldehyde) and then silver stained using a protocol compatible to mass spectrometry analysis.[19] The three best replicas for each condition were used for subsequent image analysis.

Image Analysis. Images were acquired using Image scanner UMAX (Amersham Biosciences). Gels images were analyzed by Delta2D v.4 software (Decodon, GmbH, Germany). Spot detection and normalization were performed by the automated tools of the software. To reduce the number of possible "false positives", we considered only spots with a $p < 0.02$ according to the Student's *t* test and with relative standard deviation less than 30%. The resulting list of modulated spots (70 spots) was screened considering only spots at least 2-fold up or down regulated. Spots resulted by this screening (13) were also analyzed by ImageMaster 2D Platinum v.5 software (Amersham Biosciences). After automated detection, spots were manually edited and Student's *t* test was applied. The trends of spot ratios obtained by the two software were similar.

In Gel Digestion. Differentially expressed spots were manually excised. Gel pieces were destained before digestion. After destaining they were washed first with H_2O, then with 50 mM NH_4HCO_3/Ethanol 1:1 (v/v). Gel plugs were dehydrated with pure ethanol, reduced with 10 mM DTT in 50 mM NH_4HCO_3 (1 h at 37 °C) and alkylated with 55 mM iodoacetamide in 50 mM NH_4HCO_3 (30 min at room temperature). Plugs were washed with 50 mM NH_4HCO_3, dehydrated completely. A solution of 0.01 μg/μL trypsin (Promega, Madison, WI) was added, and proteins were digested at 37 °C overnight. The

reaction was stopped by adding 1% (v/v) Trifluoroacetic acid (TFA) in H_2O.

MALDI-TOF MS Analysis. Peptides were desalted by C18 ZipTips (Millipore, Billerica, MA) and cocrystallized with a solution of 0.5 mg/mL alpha-cyano-4-hydroxycinnamic acid dissolved in Acetonitrile/0.1% (v/v) TFA in H_2O (1:1) on a Ground Steel plate (Bruker-Daltonics, Bremen, Germany) prespotted with a thin layer of 10 mg/mL alpha-cyano-4-hydroxycinnamic acid dissolved in Ethanol/Acetonitrile/0.1% (v/v) TFA in H_2O (49.5:49.5:1). Spectra were acquired with a Ultraflex III MALDI TOF/TOF spectrometer (Bruker-Daltonics). A standard peptide mixture from Bruker-Daltonics (m/z 1046.54, 1296.68, 1347.73, 1619.82, 1758.93, 2093.08, 2465.19, 2932.59, 3494.65) was used for external calibration. Acquired spectra were processed by FlexAnalysis software v3.0 (Bruker Daltonics).

Internal calibration was performed using autolysis peaks from porcine trypsin (m/z 842.509 and 2211.104). After exclusion of contaminant ions (known matrix and human keratin peaks), a database search was performed using MASCOT 2.2.03 algorithm (www.matrixscience.com) against NCBInr_20090528 database restricted to *Homo sapiens* taxonomy (8 915 381 sequences) with carbamidomethylation of cysteines as fixed modification, oxidation of methionines as variable modification, one missed cleavage site allowed for trypsin and 50 ppm as maximal tolerance. Protein scores greater than 66 were considered significant ($p < 0.05$).

MALDI-TOF MS/MS Analysis. MALDI-TOF MS/MS analysis was performed in LIFT mode. Precursor ions were selected manually. MS/MS spectra were acquired with a minimum of 4000 and a maximum of 8000 laser shots using the instrument calibration file. The precursor mass window was set automatically after the precursor ion selection. Spectra baseline subtraction, smoothing (Savitsky-Golay) and centroiding was performed by FlexAnalysis v3.0 software (Bruker Daltonics). Database search was performed setting the following criteria: maximum of one missed cleavage was allowed, the mass tolerance of precursor ions and fragments were set to 75 ppm and 0.5 Da respectively; the allowed fixed modification was carbamidomethylation on cysteine and the allowed variable modification was methionine oxidation, the taxonomy was restricted to *Homo sapiens* (8 915 381 sequences). Individual ions scores >38 indicate identity or extensive homology ($p < 0.05$).

In-Solution Digestion. Protein extracts were precipitated adding a mix of ethanol, methanol and acetone (ratio 2:1:1, v/v), dissolved in 50 mM ammonium bicarbonate pH 8.5 containing 1.2 M Urea and 1% CHAPS and sonicated. Reduction and alkylation of proteins were obtained adding DTT (10 mM) (1 h at 36 °C) and iodoacetamide (50 mM) (1 h at R.T.). Protein samples at final concentration of 1.6 μg/μL were digested with 1:20 (w/w) sequence grade trypsin (Promega, Madison, WI) at 36 °C overnight. Reactions were stopped adding 5 μL of 1%(v/v) TFA.

Expression Analysis by nLC−MS^E. Separation of tryptic peptides and subsequent qualitative ad quantitative nLC−MS^E analysis were performed by nanoACQUITY UPLC System (Waters Corp., Milford, MA) coupled to a Q-Tof Premier mass spectrometer (Waters Corp., Manchester, U.K.).

Digestion mixture was diluted 1:3 in aqueous 0.1% (v/v) formic acid and 2 μL (1 μg of protein digestion) were loaded on column for peptides separation. Prior loading, a digestion of Enolase from *Saccharomyces cerevisiae* (Waters, Corp.) was added to sample as internal standard in order to have a final concentration of 100 fmol/μL on column. Peptides were injected onto a Symmetry C18 5 μm, 180 μmX20 mm precolumn (Waters Corp.) for preconcentration and desalting and subsequently separated using a NanoEase BEH C18 1.7 μm, 75 μmX25 cm nanoscale LC column (Waters Corp.) maintained at 35 °C. Mobile phase A was water with 0.1% formic acid, and mobile phase B was 0.1% formic acid in acetonitrile. Peptides were separated with a gradient of 3−40% mobile phase B over 120 min at flow rate of 250 nL/min, followed by a gradient of 40−90% mobile phase B over 5 min and a 15 min rinse with 90% mobile phase B. The column was re-equilibrated at initial conditions for 30 min. The Q-Tof Premier mass spectrometer (Waters Corp.) was operating in "High-Low mode": it was programmed to step between low (4 eV) and high (15−40 eV) collision energies on the gas cell using a scan time of 1.5 s over 50−1990 m/z.[20] The lock mass ([Glu^1]-Fibrinopeptide B, 250 fmol/μL) was delivered from the auxiliary pump of the nanoACQUITY UPLC System (Waters Corp.) with a constant flow rate of 200 nL/min. Samples were run in triplicate.

Continuum LC−MS data were processed and searched using ProteinLynx GlobalServer v2.3 (PLGS)(Waters Corporation). The ion detection, clustering, and normalization were performed using PLGS.[21,22] Protein identifications were obtained with the embedded ion accounting algorithm of the software after searching a Swiss-Prot human database (indexed on 23 September 2008; 25 245 entries) to which the sequence of enolase from *Saccharomyces cerevisiae* (Waters Corp.) was appended. The search parameters were typically 15 ppm of tolerance for precursor ions, 20 ppm of tolerance for product ions, minimum 3 fragment ions matched per peptide, minimum 7 fragment ions matched per protein, minimum 2 peptide matched per protein, 1 missed cleavage, carbamydomethylation and oxidation of methionine as modifications. The false positive rate (FPR) of the identification algorithm is typically 3−4% with a randomized database, appended to the original one, which is five times the size of the original utilized database.[21] For quantitative analysis we considered proteins identified in at least 2 out 3 injections of the same conditions. Identified proteins displayed in the protein table were normalized against P00924 entry (Enolase *Saccharomyces cerevisiae*) while the most reproducible peptides for retention time and intensity deriving from Enolase *Saccharomyces cerevisiae* digestion (m/z 814.47, m/z 1286.7148, m/z 1578.80, m/z 1840.89) were used to normalize the EMRTs table, that is the list of peptide Exact Masses paired to their Retention Times. We considered significant only modulated proteins with a $0 < P < 0.05$ or $0.95 < P < 1$. If $0 < P < 0.05$ the likelihood of down-regulation is greater than 95%, if $0.95 < P < 1$ the likelihood of up-regulation is greater than 95%.

Immunoblot Analysis. Total protein extracts were separated on 12% SDS-PAGE and transferred to nitrocellulose membranes (Bio-Rad) using SEMI-PHOR semidry transfer unit (Amersham Biosciences). The transferred membranes were blocked with 3% low fat dry milk in TPBS (0.1% Tween20 in PBS buffer) for 1 h and incubated overnight with primary antibodies anti-Hsp70 (1:1000) (Santa Cruz Biotechnology, Santa Cruz, CA), GSTpi (1:1000) (Novocastra, Newcastle, U.K.), PRDX1 (1:5000) (Santa Cruz), Nrf2 (1:1000) (Santa Cruz), β-actin (1:5000) (Sigma), diluted in 1% low fat dry milk in TPBS. Membranes were then incubated with secondary antibody conjugated with horseradish peroxidase (Bio-Rad) for 1 h and detection was done with Enhanced Chemiluminescence Plus reagent (ECL plus, Amersham Biosciences). Experiments were performed in

triplicate. Densitometric analysis was performed by ImageJ v1.43d software.

Bioinformatics Analysis. Modulated proteins identified by proteomic analysis were further analyzed by PANTHER Classification System (http://www.pantherdb.org) and Ingenuity Pathway Analysis (www.ingenuity.com). Using the PANTHER resource, it is possible to categorize genes by their molecular functions and/or biological processes on the basis of published papers and by evolutionary relationships to predict function when experimental evidence is missing. IPA highlights protein networks or pathways starting from a continuous updated database of known protein−protein interactions based on direct (physical) and indirect (functional) associations. The algorithm gives back a probability score for each possible network. Scores of 10 or higher (negative log of the *p*-value) have a high confidence of not being generated by random chance alone, and they were the only considered in the present work.

For the data mining study, a literature search in PubMed until April 1, 2010 was performed using a search strategy designed to identify studies evaluating gene expression alterations at the level of mRNA or protein in sensitive human cell lines and their cisplatin resistant counterpart. PuMed search parameters were: ((“cisplatin” [MeSH Terms] OR “cisplatin” [All Fields]) AND resistance [All Fields]) AND (“cell line” [MeSH Terms] OR (“cell” [All Fields] AND “line” [All Fields]) OR “cell line” [All Fields]) AND (proteomic [All Fields] OR microarray [All Fields]) AND ((“2004/01/01” [EDAT]: “2010/04/01” [EDAT]) AND English [lang]). Including criteria for papers selection were: (1) comparative analysis among human cell lines sensitive to cisplatin and their resistant counterpart; (2) papers published in the last 6 years; (3) papers published in English language. Excluding criteria for papers selection were: (1) only selected genes analyzed; (2) reviews; (3) response to cisplatin treatment or other drugs (i.e., not acquired drug resistance studies) or comparison among different resistant cell lines (i.e., not comparative analysis among sensitive and resistant cell lines; (4) microRNA profiling or promotor methylation profiling; (5) Comparative genomic hybridization (CGH) analysis; (6) data partially available. Modulated genes/proteins reported in the selected papers were used to run IPA analysis (IPA version 8.5, released 2010/02/13). The resulting significant canonical pathways with a *p-value* $< 1 \times 10^{-02}$ were used to construct a qualitative binary matrix utilized for the subsequent Hierarchical Clustering Analysis, performed by PermutMatrix according to the Euclidean distance and McQuitti’s aggregation method.[23]

Enzyme Assay. After reached a 80−90% confluence in 100 × 20 mm culture disks in complete media cells were homogenized in 1 mL of 0.1 M Tris-HCl, 0.15 M KCl, 0.05%(v/v) Triton X-100, 5 mM 2-mercaptoethanol, pH 7.8, in a glass/Teflon Potter homogenizer and centrifuged at 400 000× *g* for 15 min at 4 °C. Supernatants were immediately used for glutathione peroxidase activity measurements.[24] Briefly, 0.1 to 0.8 mg of protein was used in the activity test (0.1 M Tris-HCl pH 7.8, 3 mM GSH, 0.1% Triton X-100, Glutathione Reductase 1.5 IU/mL and 30 μM NADPH). The enzyme reaction was detected at 340 nm after adding the peroxidatic substrate (50 μM H_2O_2 for Glutathione Peroxidase 1).

Immunofluorescence. Cells were fixed in methanol, rinsed with PBS and blocked for 1 h in PBS with 10% FBS. Fixed cells were incubated for 1 h with anti-Nrf2 primary antibody (1:50) (Santa Cruz) in PBS with 5% FBS, rinsed with PBS with 0,1% Tween 20 and then incubated 1 h with secondary antibody Cy3 conjugated anti rabbit IgG (1:1000) (Jackson ImmunoResearch Laboratories, Baltimore Pike, West Grove, PA). Nuclei were stained with Hoechst dye 1 μg/μL (H33258, Riedel de Haen, Hannover, Germany). The cover glasses were mounted in ProLong anti-Fade Reagent (Molecular Probes, Leiden, The Nedherlands). Analysis was performed with a confocal laser scanning microscope (SP5, Leica Microsystems, Wetzlar, Germany) using a 63× oil-objective (electronic zoom factor 2×). Three different preparations were obtained for both cell lines. A total of six random fields were acquired for each condition. Each fluorochrome was scanned individually and each image included 8−21 cells. The number of cells showing a certain pattern (e.g., Nrf2 localization) was counted in every image and expressed as a percentage of all cells in the image. Then the average values, expressed as percentage, from different images were calculated. The significance of differences was analyzed using Mann−Whitney test, $p < 0.05$ were considered significant. Acquired images of separated channels were exported using Leica Application Suite 6000 as .tiff files. Figures were generated using ImageJ v1.43d software.

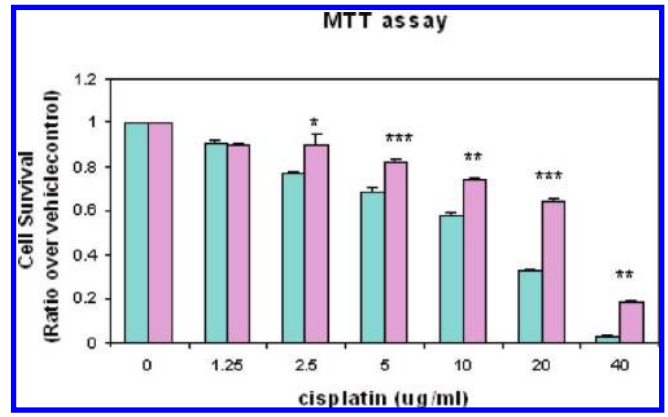

Figure 1. Cell survival measured in SH-SY5Ywt (light-blue) and SH-SY5Ycp (lilac) cells following treatment with cisplatin. Sensitive and resistant cells were maintained in media containing 10% FBS for 24 h, followed by incubation with different concentration of cisplatin for other 24 h. Cell survival was monitored by MTT analysis. Values are means + SD from three experiments. *$p < 0.05$, **$p < 0.01$, ***$p < 0.001$.

Results

Evaluation of Cisplatin Toxicity. A neuroblastoma SH-SY5Y cell line resistant to cisplatin (SH-SY5Ycp) was selected in our laboratory by exposing cells to increasing dose of drug. Cell survival of sensitive (SH-SY5Ywt) and resistant cell lines was determined by a dose−response experiment. Both cells lines were incubated with cisplatin at different concentration for 24 h and cell viability was monitored by MTT analysis (Figure 1). The calculated EC50 for the resistant cell line was 25.39 ± 2.7 μg/mL, while the EC50 for the sensitive one was 12 ± 1.8 μg/mL. In the case of the sensitive cell line it was enough a cisplatin concentration of 20 μg/mL to detect a viability minor than 40%, while at the same drug concentration the resistant cell line showed a viability higher than 60%.

Proteomic Pattern of Cisplatin Sensitive and Resistant Human Neuroblastoma Cells by 2-DE Coupled to Mass Spectrometry Analysis. To study the mechanisms of resistance to cisplatin in neuroblastoma, we compared the proteomes of a sensitive neuroblastoma cell line, SH-SY5Ywt, and its cisplatin resistant counterpart, SH-SY5Ycp. We performed the 2-DE

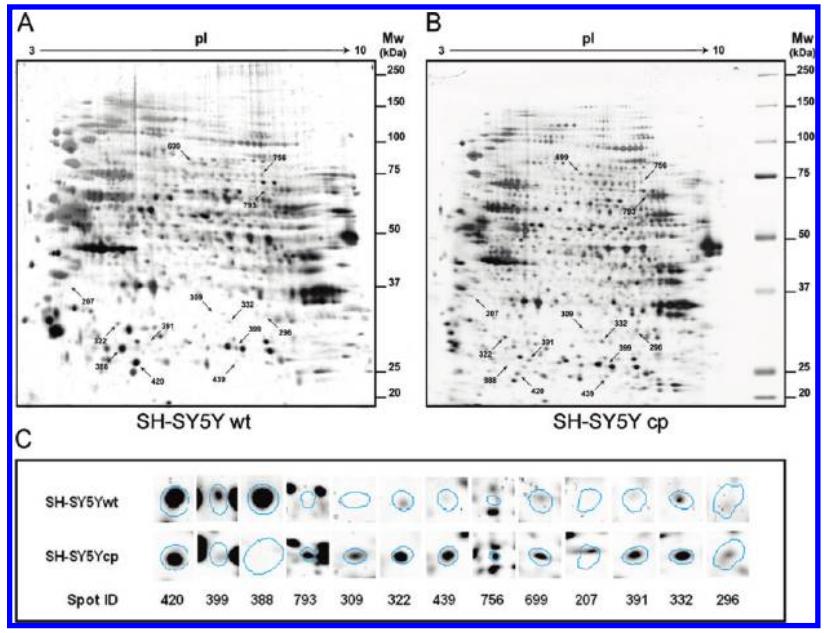

Figure 2. Proteomic comparison between (A) SH-SY5Ywt (sensitive) and (B) SH-SY5Ycp (resistant) cells by 2-DE electrophoresis. Proteins were separated using 18 cm, pH 3−10 NL strips in first dimension and a 7−14% acrylamide gradient in second dimension. After run spots were visualized by silver staining. Numbers indicate differential expressed spots identified by mass spectrometry and reported in Table 1. (C) Zoomed area corresponding to spots of interest in representative gels.

analysis of both cell lines using 18 cm gels (IPG 3−10NL) for the first dimension and 7−14% gradient polyacrylamide gels for the second dimension. Silver staining visualized more than 790 ± 50 spots from 100 μg of proteins (Figure 2 A and B). Image analysis revealed 13 differentially expressed spots (see Materials and Methods for details), with at least 2-fold increase or decrease, in a reproducible way between resistant and sensitive cell lines (Figure 2C). Spots of interest were isolated by excision, trypsin digested and analyzed by peptide mass fingerprinting (PMF) and MS/MS (Table 1). Using the NCBI database restricted to *Homo sapiens*, only one protein was identified for each spot.

Identifications listed in Table 1 showed Mascot scores a for PMF above 66, sequence coverages above 19% and peptide Mascot scores above 42.

Three spots, corresponding to glutathione S-transferase p1, triosephosphate isomerase 1, and ubiquitin carboxyl-terminal esterase L1 were found down-regulated in the resistant cell line. Ten spots were found up-regulated in the resistant cell line: peroxiredoxin 4, proteasome activator subunit 2, ezrin, DEAD/H (Asp-Glu-Ala-Asp/His) box polypeptide 3, proteasome alpha2 subunit, voltage-dependent anion channel 2/porin (VDAC2/porin), transketolase, peroxisomal enoyl-coenzyme A hydratase -like protein, proteasome alpha1 subunit isoform 2 and eukaryotic translation elongation factor 1.

Proteome Profiling by Label-free nLC−MS^E. A comparative proteome analysis of the two cell lines was also performed by nLC−MS^E. Whole-cell protein extracts were digested by trypsin and loaded on a nanoACQUITY UPLC System (Waters Corp.) coupled to a Q-TOF Premier mass spectrometer (Waters Corp.) operating in high-low mode. At least triplicate were run for each condition. Prior qualitative and quantitative analysis data quality was verified (Figure 3). Figure 3A and C shows the scatter plots of EMRT intensities for 2 replica of the same condition. In both cases, experimental points were distributed along a diagonal line. This result is evidence of good data reproducibility because it is not far from the ideal condition in which a binary comparison would yield a perfect 45-degree diagonal intersecting through zero. Moreover, for both conditions, the distribution of mass error was under 15 ppm with the greater part of peptide species under 4 ppm (B, D), the retention time coefficient of variation expressed as percentage (%CV RT) was under 4% with the greater part of peptides species under 2% (E, G) and the intensity coefficient of variation expressed as percentage (%CV intensity) has a Gaussian distribution with all values under 4.5% (F, H). After quality assessment, an EMRTs table and a protein table were generated. A total of 56 968 EMRTs and 480 proteins were qualitatively identified across both conditions. Quantitative analysis was performed after EMRTs and protein normalization. Only proteins identified in at least two out of three injections with a fold change of regulation greater than 1.5 were considered in the subsequent analysis. A fold change of 1.5 (±0.50 on a natural log scale) indicated that the significance of the regulation level was set at 50%, which is more than 3 times higher than the estimated error on the intensity measurement.

Applying these stringent filtering criteria a total of 88 significant differentially expressed proteins were highlighted (Table 2, Table 1S). Interestingly it is possible to observe a congruency in expression trends between 2-DE comparative analysis and results obtained by label-free differential analysis. In fact, ubiquitin carboxyl-terminal esterase L1, transketolase, thioredoxin peroxidase and eukaryotic elongation factor 1 showed similar trends in expression change by both proteomic approaches. Two isoforms of voltage-dependent anion channel (VDAC 1 by nLC−MS^E and VDAC 2/porin by 2-DE analysis) were found up-regulated in the cisplatin-resistant cell line. Discrepancy is found in the case of triosephosphate isomerase, which was up-regulated in the cisplatin-resistant cell line by label-free differential analysis but down-regulated according to 2-DE analysis. This result could be explained considering that in the case of 2-DE analysis differential expression among spots belonging to the same proteins may be highlighted, either when spots correspond to different amino acid sequences or

Table 1. Protein Identification by MALDI-TOF/TOF Analysis

spot ID (wt/cp)	ratio[a]	*p*-value[b]	accession number[c]	identified protein[d]	score[e]	matched peptides[f]	sequence coverage	theor. M_r/*pI*	identified peptide by MS/MS[g](score)	*m*/*z*[h]
388	29	0.02	gi|21361091	Ubiquitin carboxyl-terminal esterase L1	114	9/33	63.2%	25.2KDa/5.2	–	–
420	3.3	0.02	gi|2554831	Glutathione S-Transferase P1	88	7/27	47.6%	23.5KDa/5.4	^{2}PPYTVVYFPVR^{12} (42) ^{93}DQQEAALVDMVNDGVEDLR^{101} (42)	1337.70 2116.89
399	2.0	0.001	gi|999892	Triosephosphate Isomerase 1	66	5/21	35.9%	26.8KDa/6.5	^{33}VPADTEVVCAPPTAYIDFAR^{52} (69)	2192.08
391	0.50	0.03	gi|5453549	Peroxiredoxin 4	81	7/27	35.4%	30.7KDa/5.8	^{46}TREECHFYAGGQVYPGEASR^{66} (105)	2443.10
322	0.50	0.03	gi|30410792	Proteasome activator subunit 2	96	8/44	39.7%	27.5KDa/5.3	^{22}QNLFQEAEEFYR^{34} (80)	1686.80
699	0.50	0.001	gi|28948869	Ezrin	74	6/19	19.9%	35KDa/9.5	^{273}APDFVFYAPR^{282} (50)	1182.60
756	0.47	0.02	gi|87196351	DEAD/H (Asp-Glu-Ala-Asp/His) box polypeptide	97	11/23	19.5%	73.6KDa/6.8	-	-
439	0.45	0.01	gi|39644890	Proteasome alpha 2 subunit	78	5/19	28.2%	26KDa/7.7	-	-
296[i]	0.45	0.05	gi|48146045 (gi|190201)	Voltage-dependent anion channel 2 (VDAC2)(porin)	69	5/15	26%	30.8KDa/6.8	-	-
793	0.37	0.02	gi|31417921	Transketolase	76	7/22	25%	50.3KDa/9.0	-	-
309	0.31	0.02	gi|70995211	Peroxisomal enoyl-coenzyme A hydratase -like protein	88	6/17	32%	36.1KDa/9.1	^{215}VIGNQSLVNELAFTAR^{230} (125)	1372.04
332	0.30	0.02	gi|4506179	Proteasome alpha1 subunit isoform2	86	8/22	35.7%	29.8KDa/6.2	^{103}FVFDRPLPVSR^{113} (45) ^{4}NQYDNDVTVWSPQGR^{18} (88)	1332.69 1778.79
207	0.27	0.04	gi|25453472	Eukaryotic translation elongation factor 1 delta isoform 2	80	8/25	30%	31.2KDa/4.8	^{84}IASLEVENQSGR^{95} (87)	1358.66

[a] Ratio of percentage spot volume between SH-SY5Ywt and SH-SY5Ycp by ImageMaster 2D Platinum software; the same spots were found at least 2-fold regulated by Delta2D software. [b] *p*-value according to Student *t* test by ImageMaster 2D Platinum software; for the same spots a *p*-value < 0.02 was calculated applying Student *t* test by Delta 2D software. [c] Accession No. according to NCBI database. [d] Name of identified proteins. [e] Peptide Mass Fingerprinting score calculated by MASCOT 2.2.03 algorithm (www.matrixscience.com) after database search. [f] Number of experimental peptides matched versus searched peptides. [g] Aminoacidic sequence of the peptides identified by MS/MS analysis (with related score calculated by MASCOT 2.2.03 algorithm). [h] Monoisotopic masses of the parent ions used for MS/MS analysis. [i] In this case it was not possible to discriminate among the accession numbers reported by matching peptides: gi|48146045 VDAC 2 and gi|190201 porin [*Homo sapiens*].

when post-translational modifications cause a shift position on the gels. In the case of nLC−MS^{E}, although it may be possible to identify different isoforms with different amino acid sequences, it was not always possible to discriminate among different isoforms (with the same amino acid sequences) due to post-translational modifications. Protein expression changes observed by comparative proteomic analysis were confirmed by Western blotting for HSP70, PRDX1 and GSTpi. In all cases, the results were consistent with trends observed by 2-DE and nLC−MS^{E} (Figure 4).

In Silico Analysis of Proteins Modulated in Cisplatin-Sensitive and Resistant Neuroblastoma Cell Lines. All modulated proteins resulted by 2-DE and nLC−MS^{E} analysis were classified for their molecular functions using PANTHER Classification System (Figure 5). Most part of differential expressed proteins were represented by cytoskeletal proteins (22.3%), nucleic acid binding proteins (18.1%) and chaperones (10.6%). Oxidoreductases (6.4%), isomerases (4.3%) and select calcium binding proteins (4.3%) were also well represented. To highlight possible molecular mechanisms underling cisplatin resistance, pathway analysis was carried out on the complete data sets of modulated proteins using Ingenuity Pathway Analysis software (IPA). Known mutual interactions among differentially expressed proteins were used to construct protein networks ranked by score. The network with highest score (Figure 1S, Supporting Information) resulted being constructed mostly by up-regulated proteins in resistant cell line. Among them there were cytoskeletal proteins as tubulins (TUBA1B, TUBB, TUBB2A), alpha actinin (ACTN1), myosin (MYH9) and cytoskeletal keratin (KRT17), annexin A2 (ANXA2), a calcium binding protein, which may be involved in heat-stress response or in exocytosis, common metabolic enzymes like lactate dehydrogenase (LDHA and LDHB), glyceraldehyde-3-phosphate dehydrogenase (GAPDH), phosphoglycerate kinase 1 (PGK1) antioxidant enzymes like peroxiredoxin 1, peroxiredoxin 4 and peroxiredoxin 5 (PRDX1, PRDX4, PRDX5), proteins involved in folding like heat-shock protein 90 (HSP90) and peptidyl-prolyl *cis*−*trans* isomerase A (PPIA), a redox sensitive chaperone like PARK7, translational elongation factors and antiapoptotic and regulatory proteins like members of the 14-3-3 family.

Data Mining of Modulated Proteins in Different Cell Lines Used As Model of Cisplatin Resistance. We performed a meta-analytical study in order to evaluate the main pathways involved in other cellular models of resistance to cisplatin with different genotypes and phenotypes. Starting from a total of 71 papers (the complete list is reported in Supplemental References) we selected 13 works published in the last years in which transcriptomics and/or proteomics platforms were applied to cisplatin resistant cell lines derived from ovarian cancer, breast cancer, germ cell tumors, and squamous cell carcinoma. The lists of modulated proteins or genes reported in the selected papers were used to run IPA analysis, in which results obtained from our neuroblastoma model were also included. Among the resulting Tox lists with highest *p*-value, the most frequent were Nrf2 mediated Oxidative stress response, Oxidative stress and Aryl Hydrocarbon Receptor (AhR) Signaling, a recognized pathway involved in carcinogenesis[25] (Figure 6B). The top 10 of significant Canonical pathway were reported in a binary matrix. The resulting cluster revealed the

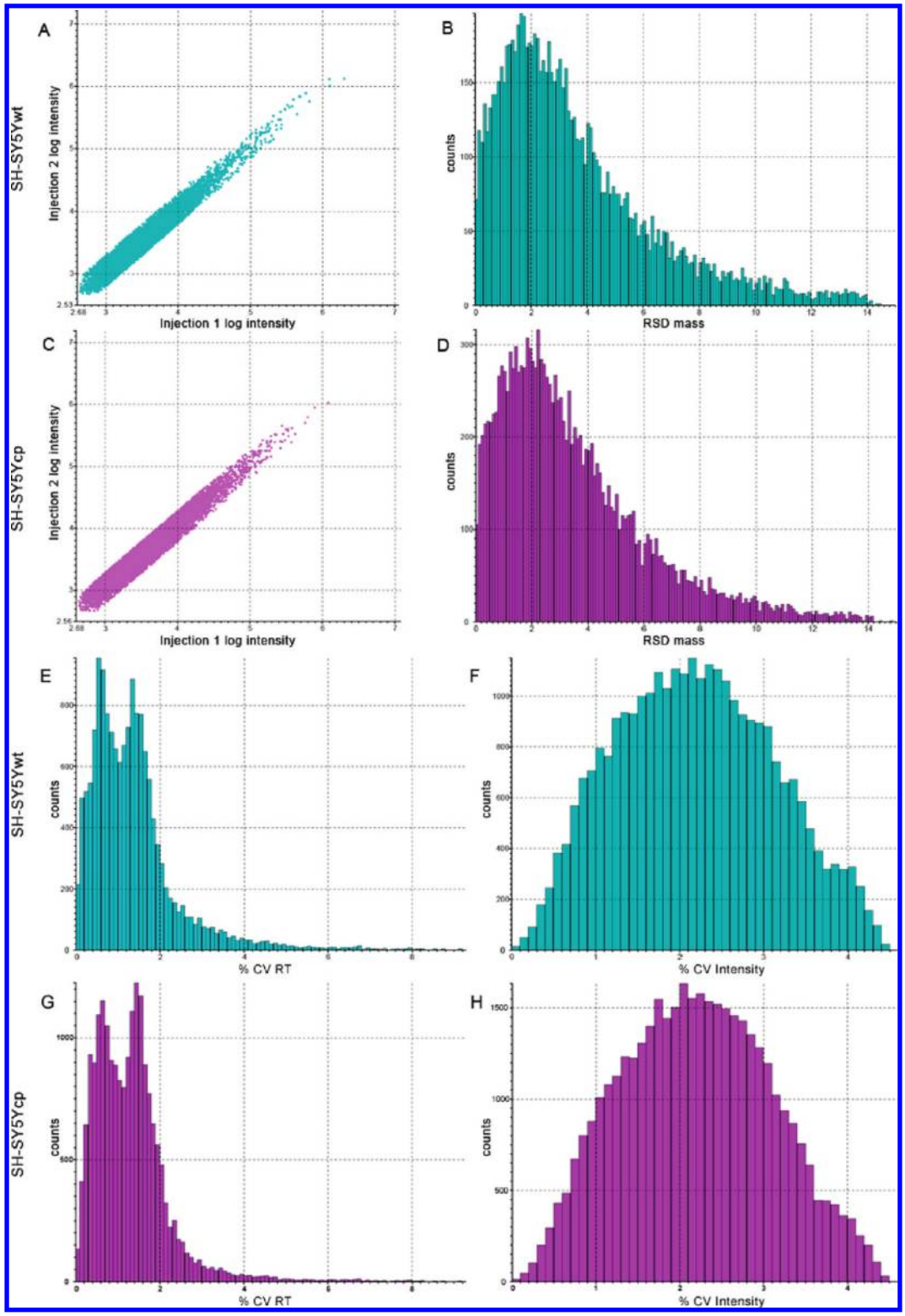

Figure 3. nLC−MS^E data quality evaluation. Analytical reproducibility assessment in SH-SY5Ywt and SH-SY5Ycp. The quality of replica was confirmed by these binary comparisons in which experimental points are distributed along a diagonal line with an inclination of about 45-degree (A, C). Bar chart showing mass precision (B, D), retention time coefficient of variation (%CV RT) (E, G) and intensity coefficient of variation (% CV intensity) (F, H) reported for EMRTs of SH-SY5Ywt and SH-SY5Ycp.

frequent occurrence of Oxidative stress response mediated by Nrf2 (Figure 6C).

Nrf2 Activation in Cisplatin-Resistant Neuroblastoma Cell Line. Possible activation of the transcription factor Nrf2 was first investigated by Western blotting (Figure 7A). Nevertheless, the modulation of Nrf2 expression was less evident when total protein extracts were compared, and the increment of Nrf2 in a resistant cell line was clearly evident when nuclei enrichment extracts were investigated (Figure 7B). We also performed confocal microscopy experiment to analyze the

Table 2. Significant Differentially Regulated Proteins in SH-SY5Ywt (SH wt) and SH-SY5Ycp (SH cp) Identified by Label-free LC−MS[E]

accession[a]	description	highly represented[b]	ratio[c]	log ratio	log std dev ratio	MW (Da)	p*I* (pH)	plgs Score
P62241	40S ribosomal protein S8	SHcp	−	−	−	24 190	10.72	151.26
P05388	60S acidic ribosomal protein P0 (L10E)	SHcp	−	−	−	34 251	5.60	189.73
P50914	60S ribosomal protein L14 (CAG-ISL 7)	SHcp	−	−	−	23 274	11.40	166.38
P05141	ADP/ATP translocase 2 (Adenine nucleotide translocator 2)	SHcp	−	−	−	32 874	10.04	165.95
P12236	ADP/ATP translocase 3 (Adenine nucleotide translocator 2)	SHcp	−	−	−	32 845	10.06	144.00
P12814	Alpha-actinin-1 (Alpha-actinin cytoskeletal isoform)	SHcp	−	−	−	102 992	5.09	438.29
P07355	Annexin A2 (Annexin II)	SHcp	−	−	−	38 579	7.78	446.16
P99999	Cytochrome c	SHcp	−	−	−	11 741	9.96	125.68
P13639	Elongation factor 2 (EF-2)	SHcp	−	−	−	95 277	6.39	877.19
P49411	Elongation factor Tu, mitochondrial precursor (EF-Tu)	SHcp	−	−	−	49 510	7.37	129.36
P14625	Endoplasmin precursor (Heat shock protein 90 kDa beta member 1)	SHcp	−	−	−	92 411	4.56	427.25
P60842	Eukaryotic initiation factor 4A-I (ATP-dependent RNA helicase eIF4A-1)	SHcp	−	−	−	46 124	5.15	230.49
P21266	Glutathione S-transferase Mu 3 (GSTM3−3)	SHcp	−	−	−	26 542	5.21	156.35
P62826	GTP-binding nuclear protein Ran (GTPase Ran)	SHcp	−	−	−	24 407	7.31	303.57
P63244	Guanine nucleotide-binding protein subunit beta 2-like 1	SHcp	−	−	−	35 054	7.56	273.28
O60812	Heterogeneous nuclear ribonucleoprotein C-like 1	SHcp	−	−	−	38 822	9.46	385.01
P38159	Heterogeneous nuclear ribonucleoprotein G (hnRNP G)	SHcp	−	−	−	42 306	10.24	201.37
P02533	Keratin, type I cytoskeletal 14 (Cytokeratin-14)	SHcp	−	−	−	51 589	4.90	381.13
Q04695	Keratin, type I cytoskeletal 17 (Cytokeratin-17)	SHcp	-	-	-	48 076	4.78	500.37
P35579	Myosin-9 (Myosin heavy chain 9)	SHcp	−	−	−	226 390	5.34	876.21
P00558	Phosphoglycerate kinase 1 (Primer recognition protein 2)	SHcp	−	−	−	44 586	8.15	538.62
P11940	Polyadenylate-binding protein 1 (Poly(A)-binding protein 1)	SHcp	−	−	−	70 625	9.81	232.06
P29401	Transketolase (TK)	SHcp	−	−	−	67 834	7.48	509.33
P22314	Ubiquitin-activating enzyme E1 (A1S9 protein)	SHcp	−	−	−	117 774	5.38	375.54
P21796	Voltage-dependent anion-selective channel protein 1 (VDAC-1)	SHcp	−	−	−	30 753	8.87	207.54
P33316	Deoxyuridine 5′-triphosphate nucleotidohydrolase	−	2.44	0.89	0.29	26 689	9.87	192.74
Q71DI3	Histone H3.2 (H3/m)		1.84	0.61	0.40	15 378	11.68	424.46
Q07021	Complement component 1 Q subcomponent-binding protein	−	0.64	−0.44	0.23	31 342	4.55	530.67
P31948	Stress-induced-phosphoprotein 1 (STI1)	−	0.63	−0.47	0.21	62 599	6.39	417.88
P19105	Myosin regulatory light chain 2, nonsarcomeric (Myosin RLC)	−	0.55	−0.59	0.41	19 781	4.45	331.95
P55209	Nucleosome assembly protein 1-like 1 (NAP-1-related protein)	−	0.55	−0.59	0.49	45 345	4.16	89.06
P27348	14-3-3 protein theta (14-3-3 protein tau)	−	0.55	−0.59	0.30	27 746	4.48	281.10
Q99497	Protein DJ-1 (Oncogene DJ1)	−	0.52	−0.65	0.25	19 878	6.37	364.15
P62937	Peptidyl-prolyl cis−trans isomerase A (PPIase A)	−	0.51	−0.67	0.12	18 000	7.85	711.03
P05455	Lupus La protein (Sjoegren syndrome type B antigen)	−	0.51	−0.67	0.47	46 808	6.75	217.35
P51858	Hepatoma-derived growth factor (HDGF)	−	0.50	−0.70	0.47	26 771	4.50	157.33
Q9Y281	Cofilin-2 (Cofilin, muscle isoform)	−	0.49	−0.72	0.24	18 724	8.16	370.07
O75531	Barrier-to-autointegration factor (Breakpoint cluster region protein 1)	−	0.49	−0.72	0.54	10 052	5.72	187.91
P30101	Protein disulfide-isomerase A3 precursor (Disulfide isomerase ER-60)	−	0.47	−0.75	0.26	56 746	5.93	332.66
P27797	Calreticulin precursor (CRP55)	−	0.45	−0.80	0.27	48 111	4.09	249.15
P50502	Hsc70-interacting protein (Hip)	−	0.44	−0.81	0.46	41 305	5.00	144.65
P31946	14-3-3 protein beta/alpha (Protein kinase C inhibitor protein 1)	−	0.41	−0.90	0.26	28 064	4.57	240.29
P07737	Profilin-1 (Profilin I)	−	0.39	−0.93	0.22	15 044	8.46	254.74
P38646	Stress-70 protein, mitochondrial precursor	−	0.36	−1.01	0.25	73 634	5.78	635.52
P30044	Peroxiredoxin-5, mitochondrial precursor (Prx-V)	−	0.36	−1.03	0.49	22 012	8.75	154.24
P37802	Transgelin-2 (SM22-alpha homologue)	−	0.35	−1.05	0.23	22 377	8.45	639.16
P60174	Triosephosphate isomerase (TIM)	−	0.35	−1.05	0.16	26 652	6.50	728.99
Q06830	Peroxiredoxin-1 (Thioredoxin peroxidase 2)	−	0.32	−1.14	0.16	22 096	8.24	503.20
P62081	40S ribosomal protein S7	−	0.31	−1.16	0.36	22 113	10.58	281.10
P63104	14-3-3 protein zeta/delta (Protein kinase C inhibitor protein 1)	−	0.30	−1.19	0.28	27 727	4.53	419.17
P11142	Heat shock cognate 71 kDa protein (Heat shock 70 kDa protein 8)	−	0.30	−1.19	0.10	70 854	5.20	1327.48
P07437	Tubulin beta chain (Tubulin beta-5 chain)	−	0.30	−1.21	0.10	49 638	4.59	1451.01
P29692	Elongation factor 1-delta (EF-1-delta)	−	0.30	−1.22	0.26	31 102	4.71	307.68
P08107	Heat shock 70 kDa protein 1 (HSP70.1)	−	0.28	−1.26	0.23	69 995	5.32	707.23
P10809	60 kDa heat shock protein, mitochondrial precursor (Hsp60)	−	0.27	−1.30	0.12	61 016	5.55	1404.91
P68363	Tubulin alpha-ubiquitous chain (Alpha-tubulin ubiquitous)	−	0.27	−1.30	0.12	50 119	4.76	1168.63
P11021	78 kDa glucose-regulated protein precursor (GRP 78)	−	0.26	−1.33	0.15	72 288	4.87	1032.17
P63261	Actin, cytoplasmic 2 (Gamma-actin)	−	0.23	−1.46	0.13	41 765	5.16	1676.49
P68366	Tubulin alpha-1 chain (Alpha-tubulin 1)	−	0.23	−1.49	0.19	49 892	4.75	785.13
P13645	Keratin, type I cytoskeletal 10 (Cytokeratin-10)	−	0.22	−1.52	0.33	59 482	4.95	524.51
Q13885	Tubulin beta-2A chain	−	0.21	−1.55	0.25	49 874	4.59	880.30
Q05524	Alpha-enolase, lung specific	−	0.20	−1.62	0.35	49 446	5.71	328.75
P35527	Keratin, type I cytoskeletal 9 (Cytokeratin-9)	−	0.19	−1.64	0.20	62 091	5.01	899.79
P06733	Alpha-enolase	−	0.19	−1.68	0.19	47 139	7.17	1143.37
P08670	Vimentin	−	0.18	−1.70	0.17	53 619	4.86	806.86
Q05639	Elongation factor 1-alpha 2 (EF-1-alpha-2)	−	0.18	−1.72	0.21	50 438	9.35	437.83
P08238	Heat shock protein HSP 90-beta (HSP 84)	−	0.16	−1.82	0.19	83 212	4.77	1230.98
P07900	Heat shock protein HSP 90-alpha (HSP 86)	−	0.15	−1.87	0.20	84 606	4.75	817.28

Table 2. Continued

accession[a]	description	highly represented[b]	ratio[c]	log ratio	log std dev ratio	MW (Da)	p*I* (pH)	plgs Score
P14618	Pyruvate kinase isozymes M1/M2 (Pyruvate kinase muscle isozyme)	–	0.15	−1.93	0.23	57 900	7.75	1247.16
P04406	Glyceraldehyde-3-phosphate dehydrogenase (GAPDH)	–	0.14	−1.95	0.19	36 030	8.70	1361.16
P07195	L-lactate dehydrogenase B chain (LDH-B)	–	0.14	−1.95	0.23	36 615	5.64	456.21
P68104	Elongation factor 1-alpha 1 (EF-1-alpha-1)	–	0.13	−2.05	0.21	50 109	9.34	631.00
P68032	Actin, alpha cardiac muscle 1 (Alpha-cardiac actin)	–	0.12	−2.13	0.97	41 991	5.07	510.29
P00338	L-lactate dehydrogenase A chain (LDH-A)	–	0.11	−2.20	0.26	36 665	8.37	562.15
P05787	Keratin, type II cytoskeletal 8 (Cytokeratin-8)	–	0.11	−2.23	0.15	53 671	5.34	1698.96
P06748	Nucleophosmin (NPM)	–	0.11	−2.33	0.23	32 554	4.44	583.40
P05783	Keratin, type I cytoskeletal 18 (Cytokeratin-18)	–	0.07	−2.61	0.28	48 028	5.17	1316.52
P09496	Clathrin light chain A (Lca)	SHwt	–	–	–	27 060	4.23	166.34
P12277	Creatine kinase B-type	SHwt	–	–	–	42 617	5.22	345.37
Q9C005	Dpy-30-like protein	SHwt	–	–	–	11 242	4.64	177.50
P30040	Endoplasmic reticulum protein ERp29 precursor (Erp31)	SHwt	–	–	–	28 975	7.28	100.76
Q15056	Eukaryotic translation initiation factor 4H (eIF-4H)	SHwt	–	–	–	27 368	7.20	126.27
P29966	Myristoylated alanine-rich C-kinase substrate (MARCKS)	SHwt	–	–	–	31 535	4.26	180.29
O15240	Neurosecretory protein VGF precursor	SHwt	–	–	–	67 246	4.56	661.70
P67809	Nuclease sensitive element-binding protein 1 (Y-box-binding protein 1)	SHwt	–	–	–	35 902	10.13	271.88
P68402	Platelet-activating factor acetylhydrolase IB subunit beta	SHwt	–	–	–	25 553	5.50	121.50
P16949	Stathmin (Phosphoprotein p19)	SHwt	–	–	–	17 291	5.65	520.10
P09936	Ubiquitin carboxyl-terminal hydrolase isozyme L1	SHwt	–	–	–	24 808	5.18	354.64

[a] Accession no. according to Swiss-Prot database. [b] Protein found highly represented in SH-SY5Ycp (SH cp) or in SH-SY5Ywt (SH wt). [c] Ratio between SH-SY5Ywt and SH-SY5Ycp. Details of proteins and peptides identification are reported in Supporting Information.

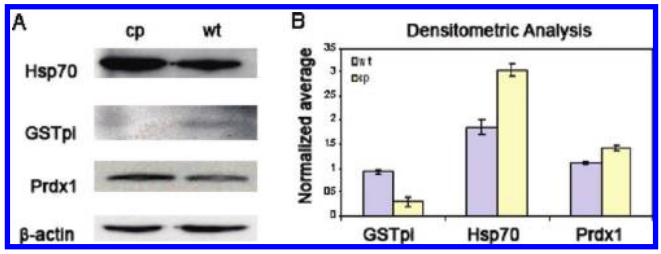

Figure 4. Immunodetections of HSP70, PRDX1, and GSTpi by Western blot of SH-SY5Ywt and SH-SY5Ycp whole lysates. (A) As suggested by nLC−MS^E and 2-DE analysis, HSP70 and PRDX1 appeared overexpressed in SH-SY5Ycp in comparison to the sensitive parental cell line. On the contrary, GSTpi appeared strongly under expressed. β-actin was used as the internal control of the protein concentration in the extracts. (B) Bar chart graph showing densitometric analysis of Western blot results after normalization. Measurements were done in triplicate and data are presented as mean + SD. Statistical analysis was performed applying the Student's *t* test. (Reported data are significant with $p < 0.05$).

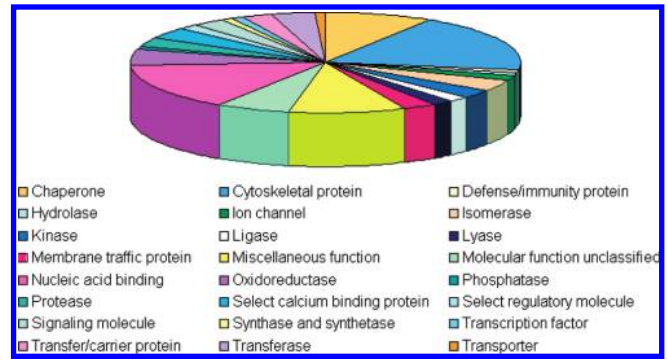

Figure 5. Molecular function classification of identified differential regulated proteins by PANTHER. The pie graph shows that a great part of modulated protein is represented by cytoskeletal proteins (22.3%), nucleic acid binding proteins (18.1%), and chaperones (10.6%).

cellular distribution of Nrf2 in the two conditions. As showed in Figure 7C, in the sensitive cell line, the signal due to Nrf2 was mostly distributed in the cytoplasm. In the case of the resistant cell line, despite of the fact that the Nrf2 signal was still localized in the cytoplasm, a number of intensely fluorescent red spots could be visualized into nucleus. The pattern resulted reproducible among the different acquired images with a significant *p*-value ($p = 0.002$) (Figure 7D). This result was in agreement with the initial hypothesis of Nrf2 activation and translocation into nuclei in the resistant cell line. Moreover, proteins that are known to be under the control of Nrf2, for example antioxidant genes like peroxiredoxins, were found modulated by our proteomic analysis, and in the case of peroxiredoxin 1, the expression change level was validated by Western blotting (Figure 4). Other evidence of the activation of Nrf2 down stream enzymes came from the measurements of glutathione peroxidase 1 activity (Figure 7E). Results revealed an increased activity in resistant cell line compared to the sensitive cell line.

Discussion

In the present work, a comparative proteomic study was carried out to identify proteins associated with cisplatin resistance in human neuroblastoma cells, allowing us to get deeper insights into the complex mechanism of the acquired resistance. For this purpose, we selected a cisplatin resistant cell line by exposing SH-SY5Y cells to a low dose of the drug. The protein profile of the resulting resistant cell line was compared to that of its sensitive counterpart by conventional proteomics using the traditional 2-DE to separate proteins, combined with mass spectrometry and database search to identify the differentially expressed proteins. This analysis highlighted the modulation of 13 proteins between the two conditions. In parallel, a more advanced approach was put in practice. A comparative proteomic investigation was also performed by label-free nLC−MS^E. This method allowed the qualitative and quantitative analysis of the total protein extracts from the two cell lines by the simultaneous screening of a large number of proteins, avoiding 2-DE separation and isotope or tag labeling of the samples.[21,22] By this approach, a total of 88 differentially expressed proteins were identified. A global

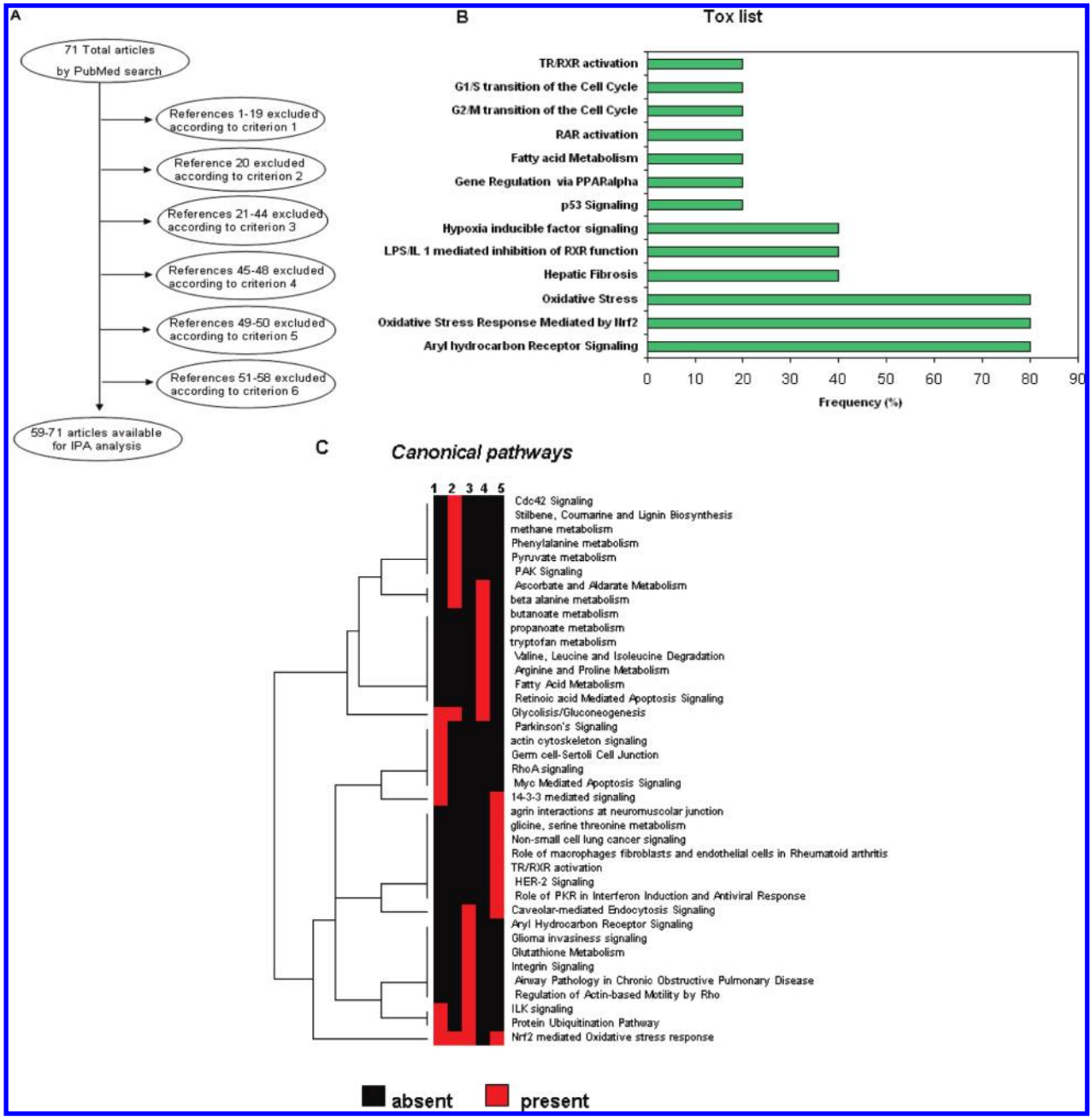

Figure 6. (A) Diagram showing working criteria. The total of 71 references resulted by PubMed interrogation (reported in Supplemental References) was screened according to 6 exclusion criteria: (1) analyzed only selected genes; (2) reviews; (3) response to cisplatin treatment or other drugs (i.e., not acquired drug resistance study) or comparison among different resistant cell lines (i.e., not comparative analysis among sensitive and resistant cell lines); (4) microRNA profiling or promotor methylation profiling; (5) Comparative genomic hybridization (CGH) analysis; and (6) data partially available. (B) Bar chart showing the frequency of most significant Tox lists found by IPA analysis. (C) Hierarchical clustering of Canonical pathways found present (red) or absent (black) in cisplatin resistant cell lines derived from neuroblastoma (1, according to our experimental data), ovarian cancer (2), breast cancer (3), germ cell tumors (4), and esophageal and oral cancer (5) according to IPA analysis of the selected published papers. Clustering was performed using the PermutMatrix software.

analysis of proteins associated with cisplatin resistance was carried out considering at the same time the results from the two proteomics approaches. By their molecular functions, modulated proteins were mostly classified into cytoskeletal proteins, nucleic acid binding proteins and chaperones. All identified proteins were considered in the further bioinformatic analysis to clarify cellular pathways underling resistance mechanism. The network reported with the highest score of probability was constructed prevalently by proteins up-regulated in the resistant cell line. Among them there were proteins implicated in cytoskeleton and cell structure, which are important for structural integrity and dynamic remodelling of cells during the development of neoplastic phenotype and execution of apoptosis like α-actinin-1, Myosin-9 and tubulin isoforms. α-Actinin-1, one of the main nodes, is a widely expressed protein that is thought to anchor actin to intracellular structures, localizing especially along cytoskeletal filaments and at focal adhesion plaques in nonmuscle cells.[26,27] Myosin-9 was

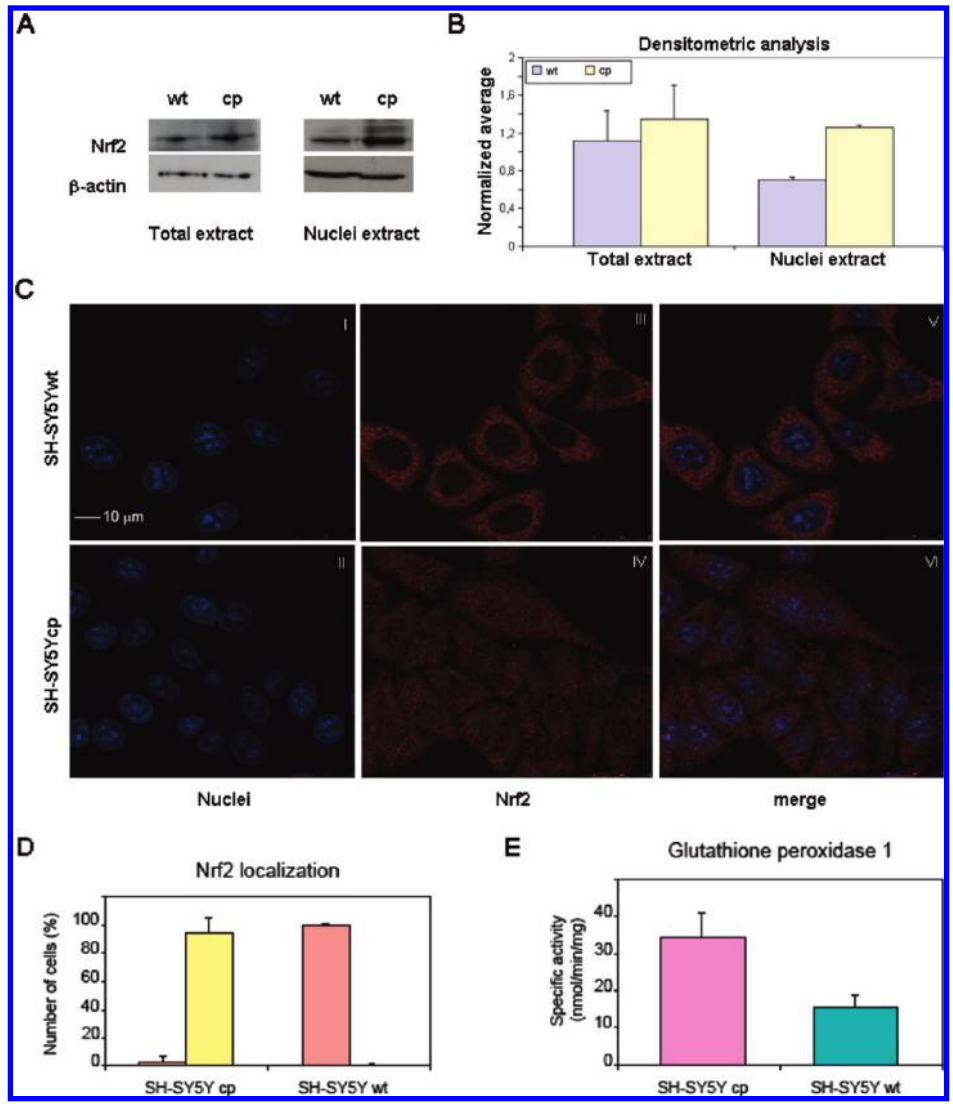

Figure 7. Nrf2 activation in SH-SY5Ycp cell line. Western blot analysis of SH-SY5Ywt and SH-SY5Ycp whole lysates with anti-Nrf2 suggested a moderated increment of Nrf2 expression level in the resistant cell line while a more evident expression is observed in extract of the enriched nuclei of resistant cell line. (A) β-actin was used as loading control. (B) Bar chart graph showing densitometric analysis of Western blot results after normalization. Measurements were done in triplicate and data are presented as mean + SD. Statistical analysis was performed applying the Student's *t* test. (Reported data are significant with $p < 0.05$). (C) Sub cellular localization of Nrf2 in SH-SY5Ywt and SH-SY5Ycp cell lines. Immunofluorescence investigation of Nfr2 localization (red) in SH-SY5Ywt and SH-SY5Ycp cells (III, IV). Cell nuclei were stained with Hoechst dye (blue) (I, II). (D) Two channels merged (V, VI). Bar chart showing the percentage of cells having different Nrf2 localization in the two conditions. Number of cells (expressed as percentage) in which Nrf2 is predominant in the cytoplasm, orange; number of cells (expressed as percentage) in which remarkable Nrf2 spots accumulate in the nuclei, yellow. The pattern resulted reproducible among the different acquired images with a significant *p*-value ($p = 0.002$). (E) Measurement of glutathione peroxidase activity. Enzyme assay results showed an increased activity of glutathione peroxidase in the resistant cell line (pink) respect to the sensitive line (green) with a significant *p*-value ($p < 0.001$) according to Mann−Whitney test.

recently associated to glioma blood vessel formation,[28] while both tubulin alpha and beta were found implicated in drug resistance to antimicrotuble agents like vincristine.[29] Several elements of the network were represented by ribosomal proteins and elongation factors, which were already described among the altered proteins in different drug resistant cancer cell lines.[8] It was reported that overexpression of 60S acidic ribosomal protein P0 might inhibit Cyclin-D1-binding protein 1 (GCIP) thus causing carcinogenesis in breast and liver tissues.[30] Moreover, chaperones and cell cycle proteins were found modulated in our analysis. Among chaperones, *in silico* analysis remarked the role of HSP90, already studied as anticancer target.[31] Since HSP90 plays a pivotal role in folding, stabilization and activation of key oncogenic client proteins such as mutant p53, ERBB2, B-RAF, C-RAF, and CDK,4[32] its selective inhibition may block malignant progression and reduce drug resistance arising.[33] A member of 14-3-3 family, 14-3-3zeta isoform, is the main node of the network. This class of proteins is implicated in cancer biology as important regulators of principal cellular processes such as proliferation, differentiation, senescence and apoptosis.[34] Among them, 14-3-3 sigma is one of the most studied. The loss of 14-3-3 sigma is a common event in breast cancer[35] and it is often associated to acquisition of drug resistance.[8] Its overexpression causes G2/M arrest, allowing the cells to repair DNA thus overcoming cell death.[36−38] Recent papers also emphasized the role of 14-3-3 zeta in tumorigenesis. Its repression sensitizes cells to stress-induced apoptosis through the activation of JNK/p38

signaling and enhances cell−cell contacts by expression of adhesion proteins.[34] Moreover, 14-3-3 zeta up-regulation was found implicated in lung,[39] breast,[35] esophageal[40] and oral cancer.[41] As expected, even redox proteins seem to be involved in the resistance mechanism. The cellular redox system may be involved in the removing of oxidants, avoiding DNA damage and apoptosis, and in DNA repair, thus explaining its modulated expression in several models of chemoresistance. We found increased levels of different peroxiredoxins, isoforms 1, 4 and 5, in the resistant cell line. These enzymes have already been described among the altered expressed proteins in resistance to different drugs, including platinum based molecules.[8,42]

Peroxiredoxins and other detoxifying enzymes essential for intracellular redox balance are controlled by the transcription factor Nrf2.[43] This consideration and the observation that the Nrf2 pathway seems to be a predominant signaling according to our *in silico* analysis suggested the possibility of Nrf2 involvement in the drug arising in the model proposed.

In normal cells, Keap1 targets Nrf2 in the cytoplasm for its degradation through the proteasome machinery, whereas in the oxidative stress condition, Nrf2 translocates into the nucleus to activate the transcription of ARE-regulated genes.[12] Keap1 also regulates the Nrf2 correct exporting from nuclei to cytoplasm when the Nrf2 function is carried out.[44] Increasing evidence suggested that three cysteine residues may be determinant for Keap1 correct function, acting as targets for electrophilic inducers of Nrf2.[45,46] Moreover, the direct phosphorylation of Nrf2 through different kinases, such as protein kinase C,[47] extracellular signal-regulated kinase 1 (ERK-1),[48] protein kinase R (PKR)-like endoplasmic reticulum kinase (PERK)[49] and tyrosine kinase Fyn,[50−52] may be relevant in the activation of this pathway.

Western blotting analysis of peroxiredoxin 1 and glutathione peroxidase activity assay are in agreement with the hypothesis of ARE gene activation in a cisplatin-resistant neuroblastoma cell line. GSTpi down-regulation found by proteomic analysis and confirmed by Western blotting can be explained considering the reported evidence according to which its transcription is not controlled by ARE element, contrary to other phase 2 detoxification enzymes.[53] Moreover Nrf2 activation was confirmed by confocal microscopy through evaluation of its increased accumulation into nuclei in the resistant cell line with respect to the sensitive one.

Nrf2 was originally studied because of its protective role in several cell conditions like inflammation,[54] neurodegenerative diseases[55,56] or aging.[57] More recently, its controversial role in cancer is emerging: Nrf2 trigger by natural or synthetic compounds may protect cells from carcinogenesis but its activation may also promote cancer.[58] The injury of the Nrf2 pathway was described in lung cancer and lung carcinoma cell lines[59,60] while Nrf2 overexpression was reported in head and neck squamous cell carcinomas.[61] Moreover, recent findings suggested that Nrf2 inhibition may render cancer cells more susceptible to chemotherapeutic drugs such as cisplatin, doxorubicin, etoposide and retinoic acid in different cell models[62,63] and in combination with carboplatin treatment may reduce tumor growth in a subcutaneous model of lung cancer.[64] Furthermore, the possible implication of Nrf2 network in resistance emergence was recently described in a cisplatin-resistant human ovarian cancer cell line.[65]

In conclusion, we performed a comparative proteomic analysis of a human neuroblastoma cell line and its derived resistant cell line by two different approaches to estimate protein functional networks involved in cisplatin resistance. As expected, chemoresistance arising is a multifactorial mechanism probably not due to a single modulated protein but to the combination of different cellular processes, whose deregulation may alter the cellular response to drug exposure. In particular, we found experimental evidence of possible Nrf2 pathway involvement in resistance to cisplatin in neuroblastoma.

Acknowledgment. We thank Fulvio Florenzano for several suggestions in the confocal experimental procedures. This work has been supported by the "Rete Nazionale di Proteomica", FIRB RBRN07BMCT Project.

Supporting Information Available: Supplementary Table 1S: Peptide table of differentially expressed proteins identified by nLC−MS^E. Figure 1S: Network analysis. Supplemental References. This material is available free of charge via the Internet at http://pubs.acs.org.

References

(1) Brodeur, G. M. *Nat. Rev. Cancer* **2003**, *3*, 203–216.
(2) Maris, J. M.; Hogarty, M. D.; Bagatell, R.; Cohn, S. L. *Lancet* **2007**, *369*, 2106–2120.
(3) Matthay, K. K.; Villablanca, J. G.; Seeger, R. C.; Stram, D. O.; et al. *N. Engl. J. Med.* **1999**, *341*, 1165–1173.
(4) Dorr, R. T.; Von Hoff, D. D. *Cancer Chemotherapy Handbook*; Appleton & Lange: Norwalk, 1994; pp 286−298.
(5) Wang, D.; Lippard, S. J. *Nat. Rev. Drug Discovery* **2005**, *4*, 307–320.
(6) Brozovic, A.; Osmak, M. *Cancer Lett.* **2007**, *251*, 1–16.
(7) Borst, P.; Rottenberg, S.; Jonkers, J. *Cell Cycle* **2008**, *7*, 1353–1359.
(8) Zhang, J. T.; Liu, Y. *Cancer Treatment Rev.* **2007**, *33*, 741–756.
(9) D'Alessandro, A.; Marzano, V.; D'Aguanno, S. *Progress in Cancer Drug Resistance Research*; Robert, A. Ed.; Nova Publishers: Parsone, 2007; pp 161−176.
(10) Urbani, A.; Poland, J.; Bernardini, S.; Bellincampi, L.; Biroccio, A.; Schnölzer, M.; Sinha, P.; Federici, G. *Proteomics* **2005**, *3*, 796–804.
(11) Copple, I. M.; Goldring, C. E.; Kitteringham, N. R.; Park, B. K. *Toxicology* **2008**, *246*, 24–33.
(12) Itoh, K.; Wakabayashi, N.; Katoh, Y.; Ishii, T.; et al. *Genes Dev.* **1999**, *13*, 76–86.
(13) Cullinan, S. B.; Gordan, J. D.; Jin, J.; Harper, J. W.; et al. *Mol. Cell. Biol.* **2004**, *24*, 8477–8486.
(14) Katsuoka, F.; Motohashi, H.; Ishii, T.; Aburatani, H.; Engel, J. D.; Yamamoto, M. *Mol. Cell. Biol.* **2005**, *25*, 8044–8051.
(15) Inamdar, N. M.; Ahn, Y. I.; Alam, J. *Biochem. Biophys. Res. Commun.* **1996**, *221*, 570–576.
(16) Kobayashi, M.; Itoh, K.; Suzuki, T.; Osanai, H.; et al. *Genes Cells* **2002**, *7*, 807–820.
(17) Moinova, H. R.; Mulcahy, R. T. *J. Biol. Chem.* **1998**, *273*, 14683–14689.
(18) Cheung, C. K.; Mak, Y. T.; Swaminathan, R. *Ann. Clin. Biochem.* **1987**, *24*, 140–144.
(19) Mortz, E.; Krogh, T. N.; Vorum, H.; Gorg, A. *Proteomics* **2001**, *1*, 1359–1363.
(20) De Canio, M.; D'Aguanno, S.; Sacchetti, C.; Petrucci, F.; Cavagni, G.; Nuccetelli, M.; Federici, G.; Urbani, A.; Bernardini, S. *J. Proteome Res.* **2009**, *9*, 4383–91.
(21) Vissers, J. P.; Langridge, J. I.; Aerts, J. M. *Mol. Cell. Proteomics.* **2007**, *6*, 755–766.
(22) Fiorentino, L.; Vivanti, A.; Cavalera, M.; Marzano, V.; Ronci, M.; Fabrizi, M.; Menini, S.; Pugliese, G.; Menghini, R.; Khokha, R.; Lauro, R.; Urbani, A.; Federici, M. *Hepatology* **2010**, *1*, 103–10.
(23) Caraux, G.; Pinloche, S. *Bioinformatics* **2005**, *21*, 1280–1281.
(24) Roveri, A.; Maiorino, M.; Ursini, F. *Methods Enzymol.* **1994**, *233*, 202–212.
(25) Puga, A.; Ma, C.; Marlowe, J. L. *Biochem. Pharmacol.* **2009**, *77*, 713–722.
(26) Lazarides, E.; Burridge, K. *Cell* **1975**, *6*, 289–298.
(27) Langanger, G.; Moeremans, M.; Daneels, G.; Sobieszek, A.; et al. *J. Cell Biol.* **1986**, *102*, 200–209.
(28) Titulaer, M. K.; Mustafa, D. A.; Siccama, I.; Konijnenburg, M.; et al. *BMC Bioinform.* **2008**, *9*, 133.
(29) Verrills, N. M.; Walsh, B. J.; Cobon, G. S.; Hains, P. G.; Kavallaris, M. *J. Biol. Chem.* **2003**, *278*, 45082–45093.

(30) Chang, T. W.; Chen, C. C.; Chen, K. Y.; Su, J. H.; et al. *Oncogene* **2008**, *27*, 332–338.
(31) Stravopodis, D. J.; Margaritis, L. H.; Voutsinas, G. E. *Curr. Med. Chem.* **2007**, *14*, 3122–3138.
(32) Whitesell, L.; Lindquist, S. L. *Nat. Rev. Cancer* **2005**, *5*, 761–772.
(33) Workman, P. *Cancer Lett.* **2004**, *206*, 149–157.
(34) Niemantsverdriet, M.; Wagner, K.; Visser, M.; Backendorf, C. *Oncogene* **2008**, *27*, 1315–1319.
(35) Neal, C. L.; Yao, J.; Yang, W.; Zhou, X.; et al. *Cancer Res.* **2009**, *69*, 3425–3432.
(36) Han, B.; Xie, H.; Chen, Q.; Zhang, J. T. *Mol. Cancer Ther.* **2006**, *5*, 903–912.
(37) Chan, T. A.; Hermeking, H.; Lengauer, C.; Kinzler, K. W.; et al. *Nature* **1999**, *401*, 616–620.
(38) Laronga, C.; Yang, H. Y.; Neal, C.; Lee, M. H. *J. Biol. Chem.* **2000**, *275*, 23106–23112.
(39) Fan, T.; Li, R.; Todd, N. W.; et al. *Cancer Res.* **2007**, *67*, 7901–7906.
(40) Bajpai, U.; Sharma, R.; Kausar, T.; Dattagupta, S.; et al. *Int. J. Biol. Markers.* **2008**, *23*, 231–237.
(41) Sawhney, M.; Matta, A.; Macha, M.A.,; Kaur, J.; et al. *Int. J. Cancer* **2009**, *124*, 2098–2105.
(42) Yan, X. D.; Pan, L. Y.; Yuan, Y.; Lang, J. H.; Mao, N. *J. Proteome Res.* **2007**, *2*, 772–780.
(43) Jaiswal, A. K. *Free Radic. Biol. Med.* **2004**, *36*, 1199–1207.
(44) Sun, Z.; Zhang, S.; Chan, J. Y.; Zhang, D. D. *Mol. Cell. Biol.* **2007**, *27*, 6334–6349.
(45) Zhang, D. D.; Hannink, M. *Mol. Cell. Biol.* **2003**, *22*, 8137–8151.
(46) Zhang, D. D.; Lo, S. C.; Cross, J. V.; Templeton, D. J.; et al. *Mol. Cell. Biol.* **2004**, *24*, 10941–10953.
(47) Bloom, D. A.; Jaiswal, A. K. *J. Biol. Chem.* **2003**, *278*, 44675–44682.
(48) Papaiahgari, S.; Zhang, Q.; Kleeberger, S. R.; Cho, H. Y.; et al. *Antioxid. Redox Signal.* **2006**, *8*, 43–52.
(49) Cullinan, S. B.; Zhang, D.; Hannink, M.; Arvisais, E.; et al. *Mol. Cell. Biol.* **2003**, *20*, 7198–7209.
(50) Jain, A. K.; Jaiswal, A. K. *J. Biol. Chem.* **2007**, *282*, 16502–16510.
(51) Kannan, S.; Jaiswal, A. K. *Cancer Res.* **2006**, *66*, 8421–8429.
(52) Salazar, M.; Rojo, A. I.; Velasco, D.; De Sagarra, R. M.; et al. *J. Biol. Chem.* **2006**, *281*, 14841–14851.
(53) Usami, H.; Kusano, Y.; Kumagai, T.; Osada, S.; et al. *J. Biol. Chem.* **2005**, *280*, 25267–25276.
(54) Braun, S.; Hanselmann, C.; Gassmann, M. G.; auf dem Keller, U.; et al. *Mol. Cell. Biol.* **2002**, *22*, 5492–5505.
(55) Chen, P. C.; Vargas, M. R.; Pani, A. K.; Smeyne, R. J.; et al. *Proc. Natl. Acad. Sci. U.S.A.* **2009**, *106*, 2933–2938.
(56) Vargas, M. R.; Johnson, D. A.; Sirkis, D. W.; Messing, A.; et al. *J. Neurosci.* **2008**, *28*, 13574–13581.
(57) Suh, J. H.; Shenvi, S. V.; Dixon, B. M.; Liu, H.; et al. *Proc. Natl. Acad. Sci. U.S.A.* **2004**, *101*, 3381–3386.
(58) Lau, A.; Villeneuve, N. F.; Sun, Z.; Wong, P. K.; Zhang, D. D. *Pharmacol. Res.* **2008**, *58*, 262–270.
(59) Singh, A.; Misra, V.; Thimmulappa, R. K.; Lee, H.; et al. *PLoS Med.* **2006**, *3*, e420.
(60) Padmanabhan, B.; Tong, K. I.; Ohta, T.; Nakamura, Y.; et al. *Mol. Cell* **2006**, *21*, 689–700.
(61) Stacy, D. R.; Ely, K.; Massion, P. P.; Yarbrough, W. G.; Hallahan, D. E.; et al. *Head Neck* **2006**, *28*, 813–818.
(62) Wang, X. J.; Sun, Z.; Villeneuve, N. F.; Zhang, S.; et al. *Carcinogenesis* **2008**, *29*, 1235–1243.
(63) Tan, K. P.; Kosuge, K.; Yang, M.; Ito, S. *Free Radic Biol Med.* **2008**, *45*, 1663–1673.
(64) Singh, A.; Boldin-Adamsky, S.; Thimmulappa, R. K.; Rath, S. K.; et al. *Cancer Res.* **2008**, *68*, 7975–7984.
(65) Cho, J. M.; Manandhar, S.; Lee, H. R.; Park, H. M.; et al. *Cancer Lett.* **2008**, *260*, 96–108.

PR100457N